Pellicle formation by Escherichia coli K-12

Golub, Stacey; Overton, Tim

DOI:
10.1016/j.jbiosc.2020.12.002

Document Version
Early version, also known as pre-print

Citation for published version (Harvard):
Golub, S & Overton, T 2021, 'Pellicle formation by *Escherichia coli* K-12: role of adhesins and motility', *Journal of Bioscience and Bioengineering*, vol. 131, no. 4, pp. 381-389. https://doi.org/10.1016/j.jbiosc.2020.12.002

PREPRINT 4-5-2020

Pellicle formation by *Escherichia coli* K-12: role of adhesins and motility

Stacey R Golub, Tim W Overton*

School of Chemical Engineering, College of Engineering and Physical Sciences and Institute of Microbiology and Infection, University of Birmingham, Edgbaston, Birmingham, B15 2TT, UK.

*to whom correspondence should be addressed: t.w.overton@bham.ac.uk, +44 (0) 121 414 5306

Keywords: motility, curli, poly-N-acetyl glucosamine, colanic acid, confocal microscopy

Short title: *E. coli* K-12 pellicles

Abstract

Initial work to generate physically robust biofilms for biocatalytic applications revealed that *Escherichia coli* K-12 can form a floating biofilm at the air-liquid interface, commonly referred to as a pellicle. Unlike other species where pellicle formation is well-characterised, such as *Bacillus subtilis*, there are few reports of *E. coli* K-12 pellicles in the literature. In order to study pellicle formation, a growth model was developed and pellicle formation was monitored over time. Mechanical forces, both motility and shaking, were shown to have effects on pellicle formation and development. The role and regulation of curli, an amyloid protein adhesin critical in *E. coli* K-12 biofilm formation, was studied by using promoter-green fluorescent protein reporters; flow cytometry and confocal laser scanning microscopy were used to monitor curli expression over time and in different locations. Curli were found to be not only crucial for pellicle formation, but heterogeneously expressed within the pellicle. The components of the extracellular polymeric substances (EPS) in pellicles were analysed by confocal microscopy using lectins, revealing distinct pellicle morphology on the air-facing and medium-facing sides,

and spatially- and temporally-regulated generation of the EPS components poly-N-acetyl glucosamine and colanic acid. We discuss the difference between pellicles formed by *E. coli* K-12, pathogenic *E. coli* strains and other species, and the relationship between *E. coli* K-12 pellicles and solid surface-attached biofilms.

Introduction

Biofilms, which can be defined as communities of microbial cells encased in a self-produced extracellular matrix, represent the most common lifestyle of bacteria on earth (1). *Escherichia coli* K-12 is non-pathogenic and commonly used as a tool in molecular biology. The formation, regulation and physiology of *E. coli* K-12 biofilms attached to solid surfaces has been well-studied (2,3). A number of surface and extracellular structures are generated by *E. coli* K-12 during biofilm formation, synthesis of which are controlled through a coordinated regulatory network (4). Flagella-mediated motility has been shown to be involved in, but not essential for, biofilm formation (3). Initial attachment to solid surfaces is primarily mediated by curli, fimbriae of several micrometers in length with amyloid characteristics (5,6,7). Type 1 fimbriae are also involved in biofilm development but not initial attachment (8). The autoagglutanin Ag43 has been shown to aid bacterial cohesion in biofilms (9).

E. coli K-12 also generates two extracellular polysaccharides as part of a biofilm matrix: Poly-N-acetylglucosamine (PNAG) (10); and colanic acid, a branched polysaccharide containing acetylated L-fucose, D-galactose, D-glucose, D-glucuronic acid, and pyruvate (11). Cellulose is not generated by most *E. coli* K-12 strains due to a stop codon in the *bscQ* gene in the operon encoding the cellulose synthesis enzymes (12).

As well as generating biofilms at solid-liquid interfaces, some species of bacteria can generate floating biofilms at air-liquid interfaces, called pellicles (13). A model of pellicle formation proposed by Armitano *et al.* suggests that bacteria first localise to the air-liquid interface, either

forming aggregates on the interface (like rafts), or extending out from the solid wall of the growth vessel (14). The cells then replicate and form a confluent pellicle across the entire air-liquid interface, followed by maturation and an increase in pellicle thickness. Pellicles have been well-characterised in the Gram positive *Bacillus subtilis*, formation being driven by motility, chemotaxis and aerotaxis (13,15). Structural components of *B. subtilis* pellicles include exopolysaccharide, TasA fibres (amyloid in nature and potentially functional homologues of *E. coli* curli (16)), and the surface hydrophobin BslA (14,17).

Although many initial reports of bacterial pellicles were in Gram-positive bacteria, some Gram-negative bacteria can also form pellicles (14). Some strains of *E. coli* have been reported to form pellicles; the greatest body of literature focuses on uropathogenic *E. coli* (UPEC) (18,19,20) and enteropathogenic *E. coli* (EPEC). Curli are known to be an important structural component of UPEC pellicles (19,21), whereas recent work determined that not all pellicle-forming EPEC strains generate curli. Unlike *E. coli* K-12, UPEC generates cellulose as a matrix component, which confers strength to UTEC pellicles (21). Recent studies have shown that transcription factor CsgD is a master regulator of pellicle formation in UPEC, activating synthesis of both curli and cellulose (22).

This study investigated the formation of pellicles by *E. coli* K-12 in terms of: the role of curli in pellicle formation; the impact of motility and other physical movement on pellicle formation; curli expression within the pellicle and within the pellicle growth model; and the EPS components within the pellicle. The results were compared to, and discussed in terms of, pellicles formed by other bacterial species and *E. coli* K-12 solid surface-attached biofilms.

Materials and methods

Strains, plasmids, and media

This study used *E. coli* K-12 strains MC4100 (*araD139Δ(argF-lac)U169 rpsL150 relA1 flbB5301 deoC1 ptsF25 rbsR*) and PHL644 (MC4100 *malA-kan ompR234)* (23). Reporter plasmid pJLC-T comprises the *E. coli* MC4100 *csgD-csgB* intergenic region upstream of the gene encoding enhanced green fluorescent protein (eGFP) with a C-terminal AANDENYALVA tag (24) cloned between the *Eco*RI-*Hin*dIII sites of pPROBE'-TT upstream of *gfp* (25), encoding tetracyclin resistance and having a pBBR1 origin of replication (26,27). Plasmid pT7-CsgD expresses CsgD under the control of a T7 promoter and confers ampicillin resistance; pT7-7 is the empty vector variant (28). Plasmids were transformed by the heat-shock method and transformants selected on Luria-Bertani-agar (10 g L^{-1} tryptone, 5 g L^{-1} yeast extract, 10 g L^{-1} NaCl, 15 g L^{-1} Bacteriological Agar; Sigma, UK) supplemented with tetracycline (10 µg mL^{-1}) or ampicillin (10 µg mL^{-1}). Untransformed strains were grown on Nutrient Agar (Oxoid) plates. Single colonies were used to inoculate 5 mL of Luria-Bertani broth (10 g L^{-1} tryptone, 5 g L^{-1} yeast extract, 10 g L^{-1} NaCl) and grown overnight (18 h, 30 °C, 150 rpm shaking) before being harvested by centrifugation (1122 g, 20 min) and resuspended in 1.4 mL of M63+ minimal medium (100 mM KH_2PO_4 (Sigma-Aldrich), 15 mM $(NH_4)_2SO_4$ (Sigma-Aldrich), 1 mM $MgSO_4$ (ThermoFisher), 1.8 µM $FeSO_4$ (Sigma-Aldrich), 10 mM D-glucose (ThermoFisher), and 17 mM sodium succinate (ThermoFisher).

Pellicle growth model and photography

To set up the pellicle growth model, 50 µL of cells from the resuspended culture grown overnight (as described above) were inoculated into test tubes containing 5 mL of M63+ minimal medium and incubated in an orbital shaker at 30 °C, 70 rpm for a period of one to six days and photographed with an Apple iPhone 5S.

Motility Assay

The OD_{600} of overnight cultures in LB medium was measured and dilutions were prepared to make the biomass concentration of each inoculum the same between strains. The diluted

culture was then point inoculated at the centre of 0.3% semisolid LB agar plates in duplicate, incubated for 24 hours at 30 °C and the distance from the inoculation point was measured.

Analysis of curli expression by flow cytometry

Cells transformed with pJLC-T were harvested from four distinct locations in the test tube (air-liquid interface, pellicle, planktonic, and sediment) at days one, two, and three. Samples were analysed using an Accuri C6 flow cytometer (BD, UK) excited using a 488 nm laser and fluorescence emission was detected using a 533/30 nm filter until 25,000 events were recorded. Mean GFP fluorescence (FL1) was calculated using CFlow software (BD, UK). As a control, the fluorescence of pPROBE-TT' in PHL644 during growth in LB and M63+ media was < 1000 units.

Pellicle visualisation by confocal microscopy

Pellicles were harvested at timepoints during maturation and mounted on microscope slides. Mounted pellicles were subsequently stained either 200 μg mL^{-1} Concanavalin A conjugated to Alexa Fluor 488 (ConA; Fisher Scientific) and incubated in darkness overnight at 4 °C, or 5 μg mL^{-1} Wheat Germ Agglutanin conjugated to FITC (WGA; Fisher Scientific) and incubated in darkness for two hours at 4 °C, and then stained with 200 µM SYTO 62 (Fisher Scientific) for 15 minutes at room temperature before visualisation. In order to ensure pellicle integrity, adhesive spacers were placed on either side of the sample so the cover slip was propped above the pellicle and contact between cover slip and pellicle was minimised. Pellicles were examined on a Lecia TCS SP8 confocal microscope equipped with a Leica DM8 CS5 Microscope (Wetzlar, Germany) with a 63x oil immersion objective lens. Optical section images and 3D images were acquired by LasX software and subsequent image analysis was performed with Fiji or imageJ software.

Genome sequencing

The genomes of strains PHL644 and PHL644h were sequenced by microbesNG (https://microbesng.uk/). Methods are described in the supplementary information.

Results and discussion

E. coli K-12 forms pellicles

Initial work focused on generating a robust, recombinant *Escherichia coli* K-12 biofilm capable of biocatalysis (29,30,31). We grew a biofilm-forming strain of *E. coli* K-12*,* PHL644, a variant of MC4100 with a mutation in the *ompR* gene (*ompR234*) resulting in increased curli expression (23), in conditions conducive to biofilm formation (M63+ minimal medium, 30 °C, and orbital shaking at 70 rpm). During efforts to optimise biofilm growth in test tubes, pellicles were observed floating at the air-liquid interface (Fig. 1A).

Macroscopic observation revealed that the floating *E. coli* K-12 pellicles were heterogeneous and appeared to vary in thickness, morphology, and structure. This observed variability continued as they formed over time from small floating aggregates to confluent layers of growth at the air-liquid interface. In order to monitor pellicle development over time, PHL644 was grown in test tubes and photographed over six days (Fig. 1B). After two days of growth, cells had begun to aggregate into “raft-like” formations at the air-liquid interface. After four days of growth, aggregates had begun to grow together into a thin pellicle and by day six, confluent pellicle growth was observed. It was also noted that cells formed solid-surface-attached biofilms on the test tube walls at the air-liquid interface, and some cells settled to the bottom of the tube forming a sediment.

Pellicle formation requires curli

PHL644, which overproduces curli, was able to generate a pellicle, however its parental strain MC4100 (carrying a wild-type *ompR* gene and synthesising less curli) did not (Fig. 1C). This

suggests that curli are important for pellicle formation in *E. coli* K-12. The importance of curli in *E. coli* K-12 pellicle formation is supported by research on UPEC pellicles. Andersson *et al*. identified chemical inhibitors of curli fibre assembly *in vitro* which also prevented pellicle formation in UPEC strain UTI89 (32); a similar effect was observed in the same study with purified *E. coli* CsgE protein, a chaperone which inhibits curli fibre assembly. Another study showed the deletion of *csgA* (encoding a curlin subunit) prevented UTI89 pellicle formation altogether (21). Wu and co-workers used varying concentrations of DMSO and ethanol to optimise curli production and thus optimised UTI89 pellicle formation (19). They also used a surfactant, Tween20, to interfere with curli interactions at the air-liquid interface and found curli and their strong entanglements were essential for pellicle formation in UTI89 (20). Likewise, atypical EPEC strain DMS9 was found to require curli for pellicle formation (33).

Pellicle formation is partially driven by motility

Some studies have shown that motility and the presence of flagella are important for pellicle formation in Gram negative bacteria (14). To investigate the effect of motility on *E. coli* K-12 pellicle formation, a hypermotile variant of PHL644 was isolated from semi-solid LB agar plates (referred to from now as PHL644h). The motility of PHL644, PHL644h, and MC4100 (parental strain) was measured (Fig. 2A), and they were found to be motile, hypermotile, and non-motile, respectively. Test tubes containing M63+ minimal medium and either PHL644 or PHL644h were grown at 30 °C and 70 rpm and pellicle formation compared (Fig. 2B). After two days, PHL644h had formed a thin pellicle and distinct solid-surface-attached biofilm on the test tube walls at the air-liquid interface while PHL644 had simply formed aggregate “rafts.” After four days, PHL644h had grown into a fully confluent pellicle of visibly greater thickness than PHL644. At six days, PHL644 had formed a fully confluent pellicle, while the PHL644h pellicle had continued to grow thicker. By day eight, both PHL644 and PHL644h had grown pellicles of substantial bulk. The growth rates of PHL644 and PHL644h in LB medium were similar over 24 hours (Supplemental Fig. S1), suggesting that the enhanced pellicle formation of PHL644h was not an effect of a growth benefit or defect.

The genomes of strains PHL644 and PHL644h were sequenced and compared. This revealed a number of mutations in PHL644h (Supplementary Table S1). A number of these mutations were in genes in the Rac prophage and DLP12 prophage; both of these prophages have been identified as being involved in motility and biofilm formation. Rac excision has been shown to be induced by biofilm formation in *E. coli* K-12, and gives rise to increased motility (34). Removal of Rac or deletion of the Rac *stfR* gene have also been shown to change *E. col* K-12 biofilm formation (34,35,36), although this is dependent upon growth medium and the molecular mechanisms underpinning this phenotype are not understood at present. Deletion of either Rac or DLP12 decreased biofilm formation in *E. coli* K-12 (36). It should be noted that regulation of motility and biofilm formation are connected; Pesavento *et al*. noted inverse regulatory coordination of motility and adhesion phenotypes in *E. coli* K-12 (37), and both flagella and curli synthesis are subject to complex, interlinked, regulation (38).

Our current hypothesis is that recombinases were induced during growth of PHL644 on semi-solid agar, giving rise to mutations in multiple locations in the hypermotile PHL644h, including in the Rac and DLP12 prophages. Prophages are known to be hotspots for genetic recombination (39) and mutations in Rac and DLP12 have previously been shown to modulate biofilm formation. The exact mechanisms by which the mutations in these prophages will be the subject of future work. However, it is clear that PHL644h is far more motile than PHL644.

Shaking contributes to pellicle formation

Localisation of bacteria to the air-liquid interface during the initial stage of pellicle formation has been shown to be influenced by both motility and passive movement, for example by shaking or Brownian motion (15,40). To further investigate the role of active motility and passive movement in *E. coli* K-12 pellicle formation, the ability of PHL644 to form pellicles with and without shaking was assessed. Test tubes containing PHL644 in M63+ minimal medium at 30 °C were either kept static for 8 days, shaken at 70 rpm for one day then kept static for seven days, or shaken at 70 rpm for 8 days (Fig. 2C). PHL644 was not able to form a mature

pellicle in static conditions after eight days: even though the typical “raft” colonies were observed at the air-liquid interface after 24 hours, pellicle maturation did not proceed. However, PHL644 tubes shaken at 70 rpm for 24 hours and then placed at static conditions for another 7 days were able to form a pellicle, albeit one less substantial than tubes shaken for eight days. This suggests that shaking enables cells to move to the air-liquid interface, “seeding” pellicle formation. While PHL644 was not able to form a pellicle in static conditions, PHL644h was able to generate a thick, confluent pellicle even without shaking (Fig 2D), suggesting that the increased motility of PHL644h eliminates the need for passive movement to the air-liquid interface.

Motility is a significant part of biofilm formation (41) and it is clear that motility and passive mobility play important roles in *E. coli* K-12 pellicle formation. Hypermotility reduces the need for passive mobility by shaking, and also confers a greater ability to form an *E. coli* K-12 pellicle in less time. In other species, motility is not always required to form a pellicle: by mutating different motility genes in *B. subtilis*, Kobayashi *et al.* revealed that a lack of motility significantly delayed pellicle formation, but did not prevent it altogether as some cells were able to use other means of passive movement or Brownian motion to eventually reach the air-liquid interface (42). This evidence suggests that while motility is important and perhaps the simplest and fastest route for the cell to overcome counteractive forces to reach the air-liquid interface, other forms of movement can localise cells to the interface where they can form a pellicle. We propose that the enhanced pellicle formation by PHL644h is due to increased swimming of PHL644h bacteria to the surface, resulting in a transfer of planktonic cells to the pellicle during pellicle development, and / or increased motility of PHL644h bacteria through the developing pellicle, enhancing pellicle development.

Curli overproduction in nonmotile MC4100

It is important to note that MC4100 (non-motile and not overproducing curli) cannot form a pellicle even when shaken (Fig. 1C), but it is unclear if lack of motility or lack of curli

overproduction is the cause. Therefore we increased curli expression in MC4100 to dissect this phenomenon. Plasmid pT7-CsgD which overexpresses the curli master regulator CsgD was transformed into MC4100; previous work showed that the effect of CsgD overexpression from this plasmid on solid surface-attached biofilm formation was comparable to that of the *ompR234* mutation carried by PHL644 in the present study (28). An empty vector, pT7-7, was transformed into MC4100 as a control. A motility assay revealed that MC4100 remained non-motile when transformed with either pT7-CsgD or pT7-7 (data not shown). MC4100 transformed with either pT7-CsgD or pT7-7 were grown in M63+ minimal medium with antibiotic, incubated at 30 °C and 70 rpm and were monitored and photographed over eight days (Fig. 3A). MC4100 transformed with pT7-7 did not grow a pellicle nor formed aggregates over the eight days. Pellicle growth in pT7-CsgD was not observed until day four, where a thin pellicle could be seen near the rear wall of the test tube. Aggregate “rafts” were visualised by day six. At day eight a thin pellicle was observed (Fig. 3B).

It should be noted that previous studies have found that the pT7-CsgD plasmid induces biofilm production in *E. coli* K-12 at least as well as the *ompR234* allele (28,31,43). Overexpression of curli in MC4100 via pT7-CsgD permitted pellicle formation in shaking conditions despite lack of motility, although pellicle formation was severely hindered when compared to PHL644 (motile) and PHL644h (hypermotile). Therefore, to produce a thick, mature pellicle a combination of curli expression, mobility, and motility are required. Overexpression of curli is required to form a pellicle and partially reduces the need for motility but not the need for mobility (shaking); shaking is required unless cells are hypermotile.

Curli formation is regulated based on location of growth within the tube

We have shown that curli are necessary to form a pellicle in *E. coli* K-12. It is known that curli expression is regulated by numerous environmental stimuli (44). To explore the regulation of curli gene expression during pellicle formation, a *csgB::gfp* reporter (pJLC-T) was transformed into PHL644. Transformants were grown in M63+ minimal medium at 30 °C and 70 rpm for

one, two or three days whereupon cells were extracted from four distinct locations within the tube and analysed by flow cytometry (Fig. 4A): air-liquid interface on the tube wall; pellicle; planktonic; and sediment. The mean GFP fluorescence which signifies the expression of *csgB* was measured for each location (Fig. 4B; individual flow cytometry histograms are shown in Supplemental Fig. S2). After one day, the pellicle and planktonic cells had high levels of *csgB* expression, while the cells at the solid surface of the air-liquid interface and the sediment at the bottom of the tube had lower expression. By day three, *csgB* expression was low in cells at the air-liquid interface (albeit after an increase on day 2), high in pellicle cells, high in planktonic cells (athough decreased from day 1), and low in sediment cells.

Curli formation is regulated in response to a variety of environmental and chemical factors including temperature, osmolarity, growth phase and carbon source (45). The *csgB* promoter is repressed by the CpxRA two-component system, which senses a variety of stimuli in the periplasm such as osmolarity and changes in pH (46), and is activated by CsgD. Expression of CsgD is mediated by multiple transcription factors including activators CRP, Cra, IHF and OmpR and repressors H-NS, CpxR and RcsAB (22,47,48), and also by multiple small RNAs (49); as such, CsgD can be considered the master regulator of curli expression, and the point of integration of multiple environmental signals. Although the *ompR234* allele in strain PHL644 increases curli expression via activation of the *csgD* promoter, expression of *csgD* and *csgA* is still responsive to environmental stimuli such as osmolarity (50) and nickel (51); the *ompR234* allele thus acts as an amplifier of curli production rather than as an overriding ‘on switch’.

Curli expression in direct response to surface attachment is suggested to be regulated by a three-component pathway: surface attachment is sensed first by outer membrane lipoprotein NIpE (52), which then activates two-component regulatory system CpxRA, which represses *csgD* and *csgB* expression and thus reduces curli formation (5,50). In addition, the difference in osmolarity experienced by planktonic cells and cells in close contact (for example in sediment) is likely to also influence *csgB* expression via the osmolarity sensor OmpR-EnvZ.

We have previously observed that sediment *E. coli* K-12 cells display lower *csgB* expression than their planktonic counterparts (27), likely to be due to sensing of osmolarity and cell-cell contact.

The downregulation of curli expression once attached to a solid surface is consistent with *csgB* expression of the cells within the tube after 24 hours in the present study; cells attached to the tube wall at the air-liquid interface and in the sediment at the bottom of the tube downregulated their curli expression when compared to planktonic or pellicle cells. The lack of solid-surface attachment in pellicle and planktonic cells result in relatively high *csgB* expression over the three days as they possibly keep producing curli while awaiting solid-surface attachment. It could also be hypothesised that curli expression remains high in pellicles due to the structural role of curli in pellicles.

Visualisation of pellicle morphology and curli at microscopic levels

To determine locations within the pellicle where the *csgB* gene was being expressed, PHL644 and PHL644h carrying the *csgB::gfp* reporter (shown as green) were analysed by confocal microscopy during maturation (Fig. 5 and Supplementary Fig. S3). Cells were counterstained with the DNA stain SYTO 62 (shown as magenta; white areas are both GFP and SYTO62 fluorescence). Morphology at the top, air-facing side of the pellicle tended to be more flat and confluent, while the bottom, medium-facing side was more irregular and formed droplet-like structures. Day 2 PHL644 pellicles were thin (ranging from 20 µm – 25 µm in thickness) with thicker regions that resembled early aggregates that were observed during previous experiments. These aggregates tended to have higher curli expression (shown in green), although other areas also expressed curli. At day 3, the pellicle had become thicker (25 µm – 35 µm) and more uniform in thickness. Curli were generally more evenly expressed throughout the pellicle, although the remnants of areas of high curli expression were still observed. After 4 days the pellicle was more homogenous in structure. Curli expression was evident throughout the pellicle with patches of higher expression. By day 6 pellicles were thicker (40

μm – 50 μm) and curli expression was limited to specific regions within the pellicle, which spanned the thickness of the pellicle top to bottom.

Taken together, curli expression is highly heterogenous within the pellicle, and changes as the pellicle develops. Pellicle thickness observed here is comparable to that of *E. coli* O55 (33). The morphological characteristics of *E. coli* K-12 pellicles observed here are also similar to those of UTEC pellicles in a study by (21), who observed that three day old pellicles had air-facing sides that were smoother and flatter and liquid-facing sides that were more irregular; however, the morphology of the top, air-facing side of *E. coli* K-12 pellicles is more complex and not as flat as that observed in UTEC. Unlike UTEC pellicles observed by Hung *et al*., *E. coli* K-12 *csgB::gfp* activity was not reduced on the liquid-facing side, rather curli expression traversed the pellicle from top to bottom.

During pellicle maturation in PHL644, overall curli expression in the pellicle as determined by flow cytometry was consistently high between days 1 and 3 (Fig. 4B), although confocal microscopy revealed that high *csgB* expression is confined to patches within the pellicle at early and late stages of development. Amyloid-rich regions within pellicles have been associated with resistance to mechanical stress (19) so it could be postulated that persistent curli production is needed to maintain pellicle structure and integrity.

Pellicles formed by PHL644h were thicker and more homogeneous in structure than those of PHL644 by 4 days of growth (Supplementary Fig. S3); in addition, they did not display the same regulation of curli as PHL644. Whereas PHL644 had specific areas of high curli expression that traversed the pellicle top to bottom much like a column, PHL644h had more even curli expression throughout the pellicle, tending to be highest in the media-facing side on day 2 and highest at the air-facing side on day 4. It is possible that because PHL644h pellicles are thicker it has more curli present throughout to increase cohesion.

Investigation of pellicle EPS

To investigate the distribution of the two polysaccharide components of the EPS, Poly-β-1,6-N-Acetylglucosamine (PNAG) and colanic acid, PHL644 pellicles at various stages of maturation were stained with fluorescently-conjugated lectins. Wheat Germ Agglutinin (WGA), conjugated to FITC, binds to N-acetyl-D-glucosamine and N-acetylneuraminic acid residues and thereby is commonly used to stain poly-*N*-acetylglucosamine (PNAG) in a variety of bacterial species. Knockouts in genes responsible for poly-*N*-acetylglucosamine synthesis in *Actinobacillus pleuropneumoniae* (53) and *Staphylococcus aureus* (54) led to a lack of WGA binding. Concanavalin A (ConA), conjugated to Alexa Fluor 488, binds to α-mannose and α-glucose (55) and thus was used to stain colanic acid which contains glucose.

Pellicles were counterstained with SYTO 62 as a DNA stain (shown in magenta versus green for the lectins) and visualised by confocal microscopy (Fig. 6). It was observed that the presence of both colanic acid and PNAG increased over time as the pellicle matured. WGA stained throughout the pellicle while ConA tended to stain the periphery of pellicle growth more. Colanic acid has previously been identified as being dispensable for adhesion but forming a protective capsule around *E. coli* biofilms (2), which could also be occurring in *E. coli* pellicles and explain why ConA tends to stain the periphery of the pellicle. Conversely, PNAG is proposed to function as a cell-cell and cell-surface adhesin and stabilise *E. coli* biofilms (56,57) and therefore is more likely to be present throughout pellicles.

EPS production in PHL644h pellicles was also investigated (Supplementary Fig. S4); it was concluded that more EPS was produced, and earlier in pellicle development, in PHL644h than PHL644. Similarly to PHL644, WGA stained PHL644h throughout the pellicle, while ConA stained the periphery of the PHL644h pellicle. It was noted that the thickness of the pellicles had inherent variability, possibly due to pellicle harvesting techniques, stain incubation times, or the heterogeneous nature of pellicles.

Conclusions

Pellicle formation in *E. coli* K-12 was shown to be dependent upon the adhesin curli and cellular movement, either provided by motility or shaking of the growth vessel; hypermotility was shown to eliminate the need for shaking. The observation that shaking is important during early stages of pellicle formation suggests that pellicles are 'seeded' by surface-associated cells that later develop into a mature pellicle. Curli expression was observed to be lower in solid surface-attached biofilms at the air-liquid interface than pellicles. We postulate that higher curli expression in pellicles is due to curli being an important structural component of pellicles, maintaining cell-cell attachment during pellicle development, whereas curli can be downregulated in biofilms once attached to a solid surface. Confocal microscopy revealed that curli expression changes over time and spatially in developing pellicles, and is different in normally motile and hypermotile *E. coli* PHL644 pellicles. Finally, pellicles appear to contain both PNAG (located throughout the pellicle) and colanic acid (located mainly on the periphery of the pellicle). Taken together, *E. coli* K-12 pellicles appear to share structural characteristics of both *B. subtilis* and UPEC pellicles and *E. coli* solid surface-attached biofilms. Future research will focus on the stimuli and pathways that regulate synthesis of curli and EPS components during pellicle and biofilm development.

Acknowledgements

Genome sequencing was provided by MicrobesNG (http://www.microbesng.uk), which is supported by the UK Biotechnology and Biological Sciences Research Council (BBSRC grant number BB/L024209/1). We thank Paolo Landini for pT7-CsgD and pT7-7 and James Leech for pJLC-T. We are extremely grateful to Alessandro Di Maio at the Birmingham Advanced Light Microscopy facility for confocal microscopy assistance and Charles Penn for discussions regarding hypermotility.

REFERENCES

1. **Flemming, H., Wingender, J., Szewzyk, U., Steinberg, P., Rice, S. A. and Kjelleberg, S.:** Biofilms: an emergent form of bacterial life, Nature Reviews Microbiology, **14,** 563 (2016).

2. **Beloin, C., Roux, A. and Ghigo, J.:** *Escherichia coli* biofilms, p. 249-289. *In* , Bacterial Biofilms. Springer (2008).

3. **Van Houdt, R. and Michiels, C. W.:** Role of bacterial cell surface structures in *Escherichia coli* biofilm formation, Res. Microbiol., **156,** 626-633 (2005).

4. **Wood, T. K.:** Insights on Escherichia coli biofilm formation and inhibition from whole-transcriptome profiling, Environ. Microbiol., **11,** 1-15 (2009).

5. **Barnhart, M. M. and Chapman, M. R.:** Curli biogenesis and function, Annu. Rev. Microbiol., **60,** 131-147 (2006).10.1146/annurev.micro.60.080805.142106.

6. **DeBenedictis, E. P., Liu, J. and Keten, S.:** Adhesion mechanisms of curli subunit CsgA to abiotic surfaces, Science advances, **2,** e1600998 (2016).

7. **Van Gerven, N., Klein, R. D., Hultgren, S. J. and Remaut, H.:** Bacterial amyloid formation: structural insights into curli biogensis, Trends Microbiol., **23,** 693-706 (2015).

8. **Rodrigues, D. F. and Elimelech, M.:** Role of type 1 fimbriae and mannose in the development of *Escherichia coli* K12 biofilm: from initial cell adhesion to biofilm formation, Biofouling, **25,** 401-411 (2009).

9. **Danese, P. N., Pratt, L. A., Dove, S. L. and Kolter, R.:** The outer membrane protein, antigen 43, mediates cell- to- cell interactions within *Escherichia coli* biofilms, Mol. Microbiol., **37,** 424-432 (2000).

10. **Cerca, N. and Jefferson, K. K.:** Effect of growth conditions on poly-N-acetylglucosamine expression and biofilm formation in *Escherichia coli*, FEMS Microbiol. Lett., **283,** 36-41 (2008).10.1111/j.1574-6968.2008.01142.x.

11. **Danese, P. N., Pratt, L. A. and Kolter, R.:** Exopolysaccharide production is required for development of *Escherichia coli* K-12 biofilm architecture, J. Bacteriol., **182,** 3593-3596 (2000).

12. **Serra, D. O., Richter, A. M. and Hengge, R.:** Cellulose as an architectural element in spatially structured *Escherichia coli* biofilms, J. Bacteriol., **195,** 5540-5554 (2013).

13. **Vlamakis, H., Chai, Y., Beauregard, P., Losick, R. and Kolter, R.:** Sticking together: building a biofilm the *Bacillus subtilis* way, Nature Reviews Microbiology, **11,** 157 (2013).

14. **Armitano, J., Méjean, V. and Jourlin- Castelli, C.:** Gram- negative bacteria can also form pellicles, Environmental Microbiology Reports, **6,** 534-544 (2014).10.1111/1758-2229.12171.

15. **Hölscher, T., Bartels, B., Lin, Y., Gallegos-Monterrosa, R., Price-Whelan, A., Kolter, R., Dietrich, L. E. P. and Kovács, Á T.:** Motility, Chemotaxis and Aerotaxis Contribute to Competitiveness during Bacterial Pellicle Biofilm Development, J. Mol. Biol., **427,** 3695-3708 (2015).10.1016/j.jmb.2015.06.014.

16. **Romero, D., Aguilar, C., Losick, R. and Kolter, R.:** Amyloid fibers provide structural integrity to *Bacillus subtilis* biofilms, Proc. Natl. Acad. Sci. U. S. A., **107,** 2230-2234 (2010).10.1073/pnas.0910560107.

17. **Hobley, L., Ostrowski, A., Rao, F. V., Bromley, K. M., Porter, M., Prescott, A. R., MacPhee, C. E., van Aalten, Daan M. F. and Stanley-Wall, N. R.:** BslA is a self-assembling bacterial hydrophobin that coats the *Bacillus subtilis* biofilm, Proc. Natl. Acad. Sci. U. S. A., **110,** 13600-13605 (2013).10.1073/pnas.1306390110.

18. **Lim, J. Y., May, J. M. and Cegelski, L.:** Dimethyl sulfoxide and ethanol elicit increased amyloid biogenesis and amyloid-integrated biofilm formation in *Escherichia coli*, Appl. Environ. Microbiol., **78,** 3369-3378 (2012).10.1128/AEM.07743-11.

19. **Wu, C., Lim, J. Y., Fuller, G. G. and Cegelski, L.:** Quantitative analysis of amyloid-integrated biofilms formed by uropathogenic *Escherichia coli* at the air-liquid interface, Biophys. J., **103,** 464-471 (2012).10.1016/j.bpj.2012.06.049.

20. **Wu, C., Lim, J. Y., Fuller, G. G. and Cegelski, L.:** Disruption of *Escherichia coli* amyloid-integrated biofilm formation at the air-liquid interface by a polysorbate surfactant, Langmuir, **29,** 920-926 (2013).10.1021/la304710k.

21. **Hung, C., Zhou, Y., Pinkner, J. S., Dodson, K. W., Crowley, J. R., Heuser, J., Chapman, M. R., Hadjifrangiskou, M., Henderson, J. P. and Hultgren, S. J.:** *Escherichia*

coli biofilms have an organized and complex extracellular matrix structure, MBio, **4,** 645 (2013).10.1128/mBio.00645-13.

22. **Hufnagel, D. A., Evans, M. L., Greene, S. E., Pinkner, J. S., Hultgren, S. J. and Chapman, M. R.:** The Catabolite Repressor Protein-Cyclic AMP Complex Regulates *csgD* and Biofilm Formation in Uropathogenic *Escherichia coli*, J. Bacteriol., **198,** 3329-3334 (2016).10.1128/JB.00652-16.

23. **Vidal, O., Longin, R., Prigent-Combaret, C., Dorel, C., Hooreman, M. and Lejeune, P.:** Isolation of an *Escherichia coli* K-12 mutant strain able to form biofilms on inert surfaces: involvement of a new *ompR* allele that increases curli expression, J. Bacteriol., **180,** 2442-2449 (1998).

24. **Andersen, J. B., Sternberg, C., Poulsen, L. K., Bjorn, S. P., Givskov, M. and Molin, S.:** New unstable variants of green fluorescent protein for studies of transient gene expression in bacteria, Appl. Environ. Microbiol., **64,** 2240-2246 (1998).

25. **Miller, W. G., Leveau, J. H. and Lindow, S. E.:** Improved *gfp* and *inaZ* broad-host-range promoter-probe vectors, Mol. Plant Microbe Interact., **13,** 1243-1250 (2000).10.1094/MPMI.2000.13.11.1243.

26. **Leech, J. T.:** Development of an *Escherichia coli* biofilm platform for use in biocatalysis.University of Birmingham (2018).

27. **Leech, J. T., Golub, S. R., Allan, W., Simmons, M. J. and Overton, T. W.:** Non-pathogenic *Escherichia coli* biofilms: effects of growth conditions and surface properties on structure and curli gene expression. , Accepted by Archives of Microbiology, (2020).10.1007/s00203-020-01864-5.

28. **Brombacher, E., Baratto, A., Dorel, C. and Landini, P.:** Gene expression regulation by the Curli activator CsgD protein: modulation of cellulose biosynthesis and control of negative determinants for microbial adhesion, J. Bacteriol., **188,** 2027-2037 (2006).10.1128/JB.188.6.2027-2037.2006.

29. **Tsoligkas, A. N., Winn, M., Bowen, J., Overton, T. W., Simmons, M. J. H. and Goss, R. J. M.:** Engineering Biofilms for Biocatalysis, Chembiochem : a European journal of chemical biology, **12,** 1391-1395 (2011).10.1002/cbic.201100200.

30. **Tsoligkas, A. N., Bowen, J., Winn, M., Goss, R. J. M., Overton, T. W. and Simmons, M. J. H.:** Characterisation of spin coated engineered *Escherichia coli* biofilms using atomic force microscopy, Colloids Surf B Biointerfaces, **89,** 152-160 (2012).10.1016/j.colsurfb.2011.09.007.

31. **Perni, S., Preedy, E. C., Landini, P. and Prokopovich, P.:** Influence of *csgD* and *ompR* on Nanomechanics, Adhesion Forces, and Curli Properties of *E. coli*, Langmuir, **32,** 7965-7974 (2016).10.1021/acs.langmuir.6b02342.

32. **Andersson, E. K., Bengtsson, C., Evans, M. L., Chorell, E., Sellstedt, M., Lindgren, A. E. G., Hufnagel, D. A., Bhattacharya, M., Tessier, P. M., Wittung-Stafshede, P., Almqvist, F. and Chapman, M. R.:** Modulation of curli assembly and pellicle biofilm formation by chemical and protein chaperones, Chem. Biol., **20,** 1245-1254 (2013).10.1016/j.chembiol.2013.07.017.

33. **Weiss-Muszkat, M., Shakh, D., Zhou, Y., Pinto, R., Belausov, E., Chapman, M. R. and Sela, S.:** Biofilm formation by and multicellular behavior of *Escherichia coli* O55:H7, an atypical enteropathogenic strain, Appl. Environ. Microbiol., **76,** 1545-1554 (2010).10.1128/AEM.01395-09.

34. **Liu, X., Li, Y., Guo, Y., Zeng, Z., Li, B., Wood, T. K., Cai, X. and Wang, X.:** Physiological Function of Rac Prophage During Biofilm Formation and Regulation of Rac Excision in *Escherichia coli* K-12, Scientific reports, **5,** 16074 (2015).10.1038/srep16074.

35. **Domka, J., Lee, J., Bansal, T. and Wood, T. K.:** Temporal gene-expression in *Escherichia coli* K-12 biofilms, Environmental microbiology, **9,** 332-346 (2007).10.1111/j.1462-2920.2006.01143.x.

36. **Wang, X., Kim, Y., Ma, Q., Hoon Hong, S., Pokusaeva, K., Sturino, J. M. and Wood, T. K.:** Cryptic prophages help bacteria cope with adverse environments, Nature Communications, **1,** 147 (2010).10.1038/ncomms1146.

37. **Pesavento, C., Becker, G., Sommerfeldt, N., Possling, A., Tschowri, N., Mehlis, A. and Hengge, R.:** Inverse regulatory coordination of motility and curli-mediated adhesion in *Escherichia coli*, Genes & development, **22,** 2434-2446 (2008).10.1101/gad.475808.

38. **Guttenplan, S. B. and Kearns, D. B.:** Regulation of flagellar motility during biofilm formation, FEMS Microbiol. Rev., **37,** 849-871 (2013).10.1111/1574-6976.12018.

39. **Ramisetty, B. C. M. and Sudhakari, P. A.:** Bacterial 'Grounded' Prophages: Hotspots for Genetic Renovation and Innovation, Front. Genet., **10,** (2019).10.3389/fgene.2019.00065.

40. **Li, G., Tam, L. and Tang, J. X.:** Amplified effect of Brownian motion in bacterial near-surface swimming, Proc. Natl. Acad. Sci. U. S. A., **105,** 18355-18359 (2008).10.1073/pnas.0807305105.

41. **Pratt, L. A. and Kolter, R.:** Genetic analysis of *Escherichia col*i biofilm formation: roles of flagella, motility, chemotaxis and type I pili, Mol. Microbiol., **30,** 285-293 (1998).

42. **Kobayashi, K.:** *Bacillus subtilis* pellicle formation proceeds through genetically defined morphological changes, J. Bacteriol., **189,** 4920-4931 (2007).10.1128/JB.00157-07.

43. **Hackett, L. D.:** Viability of engineered biocatalysts in biotransformation.University of Birmingham (2014).

44. **Smith, D. R., Price, J. E., Burby, P. E., Blanco, L. P., Chamberlain, J. and Chapman, M. R.:** The Production of Curli Amyloid Fibers Is Deeply Integrated into the Biology of *Escherichia coli*, Biomolecules, **7,** (2017).10.3390/biom7040075.

45. **Evans, M. L. and Chapman, M. R.:** Curli biogenesis: order out of disorder, Biochim. Biophys. Acta, **1843,** 1551-1558 (2014).10.1016/j.bbamcr.2013.09.010.

46. **Jubelin, G., Vianney, A., Beloin, C., Ghigo, J., Lazzaroni, J., Lejeune, P. and Dorel, C.:** CpxR/OmpR interplay regulates curli gene expression in response to osmolarity in *Escherichia coli*, J. Bacteriol., **187,** 2038-2049 (2005).10.1128/JB.187.6.2038-2049.2005.

47. **Ogasawara, H., Yamada, K., Kori, A., Yamamoto, K. and Ishihama, A.:** Regulation of the *Escherichia coli csgD* promoter: interplay between five transcription factors, Microbiology (Reading, Engl.), **156,** 2470-2483 (2010).10.1099/mic.0.039131-0.

48. **Gerstel, U., Park, C. and Römling, U.:** Complex regulation of csgD promoter activity by global regulatory proteins, Mol. Microbiol., **49,** 639-654 (2003).

49. **Andreassen, P. R., Pettersen, J. S., Szczerba, M., Valentin-Hansen, P., Møller-Jensen, J. and Jørgensen, M. G.:** sRNA-dependent control of curli biosynthesis in *Escherichia coli*: McaS directs endonucleolytic cleavage of *csgD* mRNA, Nucleic Acids Res., **46,** 6746-6760 (2018).10.1093/nar/gky479.

50. **Prigent-Combaret, C., Brombacher, E., Vidal, O., Ambert, A., Lejeune, P., Landini, P. and Dorel, C.:** Complex regulatory network controls initial adhesion and biofilm formation in *Escherichia coli* via regulation of the *csgD* gene, J. Bacteriol., **183,** 7213-7223 (2001).10.1128/JB.183.24.7213-7223.2001.

51. **Perrin, C., Briandet, R., Jubelin, G., Lejeune, P., Mandrand-Berthelot, M., Rodrigue, A. and Dorel, C.:** Nickel promotes biofilm formation by *Escherichia coli* K-12 strains that produce curli, Appl. Environ. Microbiol., **75,** 1723-1733 (2009).10.1128/AEM.02171-08.

52. **Otto, K. and Silhavy, T. J.:** Surface sensing and adhesion of *Escherichia coli* controlled by the Cpx-signaling pathway, Proc. Natl. Acad. Sci. U. S. A., **99,** 2287-2292 (2002).10.1073/pnas.042521699.

53. **Hathroubi, S., Hancock, M. A., Bossé, J. T., Langford, P. R., Tremblay, Y. D. N., Labrie, J. and Jacques, M.:** Surface Polysaccharide Mutants Reveal that Absence of O Antigen Reduces Biofilm Formation of Actinobacillus pleuropneumoniae, Infect. Immun., **84,** 127-137 (2016).10.1128/IAI.00912-15.

54. **Lin, M. H., Shu, J. C., Lin, L. P., Chong, K. y., Cheng, Y. W., Du, J. F. and Liu, S.:** Elucidating the Crucial Role of Poly N-Acetylglucosamine from Staphylococcus aureus in Cellular Adhesion and Pathogenesis, PLOS ONE, **10,** e0124216 (2015).

55. **Ghazarian, H., Idoni, B. and Oppenheimer, S. B.:** A glycobiology review: carbohydrates, lectins and implications in cancer therapeutics, Acta Histochem., **113,** 236-247 (2011).10.1016/j.acthis.2010.02.004.

56. **Wang, X., Preston, J. F. and Romeo, T.:** The *pgaABCD* locus of *Escherichia coli* promotes the synthesis of a polysaccharide adhesin required for biofilm formation, J. Bacteriol., **186,** 2724-2734 (2004).10.1128/jb.186.9.2724-2734.2004.

57. **Agladze, K., Wang, X. and Romeo, T.:** Spatial periodicity of *Escherichia coli* K-12 biofilm microstructure initiates during a reversible, polar attachment phase of development and requires the polysaccharide adhesin PGA, J. Bacteriol., **187,** 8237-8246 (2005).10.1128/JB.187.24.8237-8246.2005.

FIGURE LEGENDS

Figure 1. (A) **Initial observation of a pellicle.** *E. coli* strain PHL644 was grown in M63+ minimal medium at 30° C for six days with shaking at 70 rpm. A pellicle was observed at the surface of the medium. (B) **Timescale of *E. coli* PHL644 pellicle formation.** After two days growth, aggregates, or "rafts" formed at the surface of the medium. After four days, aggregates had grown together. At day six confluent pellicle growth was observed. (C) **Timescale of *E. coli* MC4100 pellicle formation.** After six days, *E. coli* MC4100 (which does not overexpress curli) was not able to form a pellicle.

Figure 2. (A) **Motility on semisolid agar.** A hypermotile variant of *E. coli* strain PHL644 (PHL644h) was isolated and cultured in M63+ medium. *E. coli* strains PHL644, PHL644h, and MC4100 were grown in LB at 30 °C for 24 hours with shaking at 150 rpm, then point inoculated on semisolid agar in duplicate and grown for 24 hours at 30 °C. The diameter of the growth zone was measured; error bars represent 1 standard deviation from the mean measurements of duplicate agar plates. (B) **Effect of motility on pellicle formation.** PHL644h pellicle formation was compared to the normally motile PHL644. (C) **Effect of agitation on pellicle formation.** *E. coli* PHL644 was grown in M63+ medium at 30 °C for eight days either: statically; with 70 rpm agitation for one day and then statically for seven days; or with 70 rpm agitation for eight days. (D) **Effect of agitation on pellicle formation in hypermotile cells.** *E. coli* PHL644h was able to form a pellicle in M63+ medium at 30 °C in static conditions.

Figure 3. (A) **Effect of curli overproduction in *E. coli* MC4100.** Strain MC4100 transformed with either pT7-CsgD (overproducing curli) or pT7-7 (empty vector) were grown in M63+ medium at 30 °C with 70 rpm agitation for eight days. (B) Photograph of MC4100 pT7-CsgD day eight pellicle enlarged for detail.

Figure 4. Measurement of curli promoter activity in pellicles and other cells. (A) Four distinct locations of cells sampled in this experiment. (B) Measuring curli promoter activity in four distinct locations in the system. *E. coli* PHL644 pJLC-T (carrying a *csgB::gfp* fusion) was grown in M63+ medium at 30 °C and 70 rpm for three days. Samples were taken from four locations in (A) and analysed by flow cytometry; mean green fluorescence was measured representing *csgB* promoter activity. Error bars represent 1 standard deviation from the mean of three technical replicates measured from two experimental replicates. Statistical analysis was performed by paired t test (comparison of data for same condition and different days; bars on chart) and unpaired t test of unequal variances (comparison of different locations for the same day; table); * = $p < 0.05$, NS = $p > 0.05$.

Figure 5. Visualisation of PHL644 curli production by confocal microscopy. *E. coli* PHL644 pJLC-T was grown in M63+ medium at 30 °C and 70 rpm for six days. Pellicles were harvested, stained with DNA stain SYTO62 (magenta) and visualised by confocal microscopy on days 2, 3, 4 and 6; green represents GFP. Representative single plane images from the top (air-facing), middle, and bottom (media-facing) of each pellicle as well as the side view are shown.

Figure 6. Visualisation of PHL644 EPS production by confocal microscopy. *E. coli* PHL644 was grown in M63+ medium at 30 °C and 70 rpm for six days, pellicles were harvested, stained with DNA stain SYTO62 (magenta) and either (a) WGA-FITC (stains PNAG, shown as green) or (b) ConA-Alexa Fluor 488 (stains colanic acid, shown as green) and visualised by confocal microscopy on days 2, 3, 4 and 6. Representative single plane images from each pellicle as well as the side view are shown.

FIGURE 1

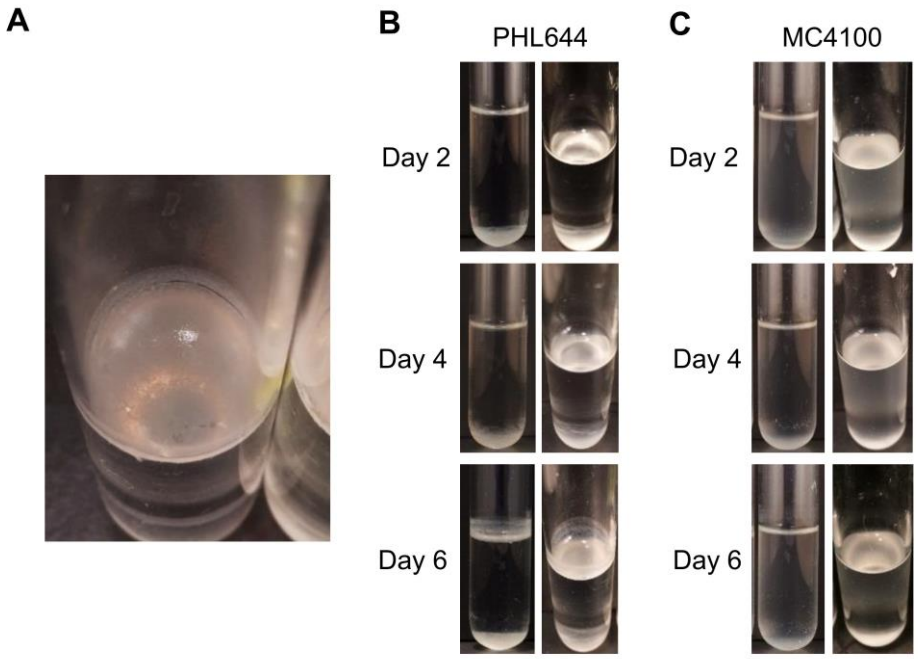

FIGURE 2

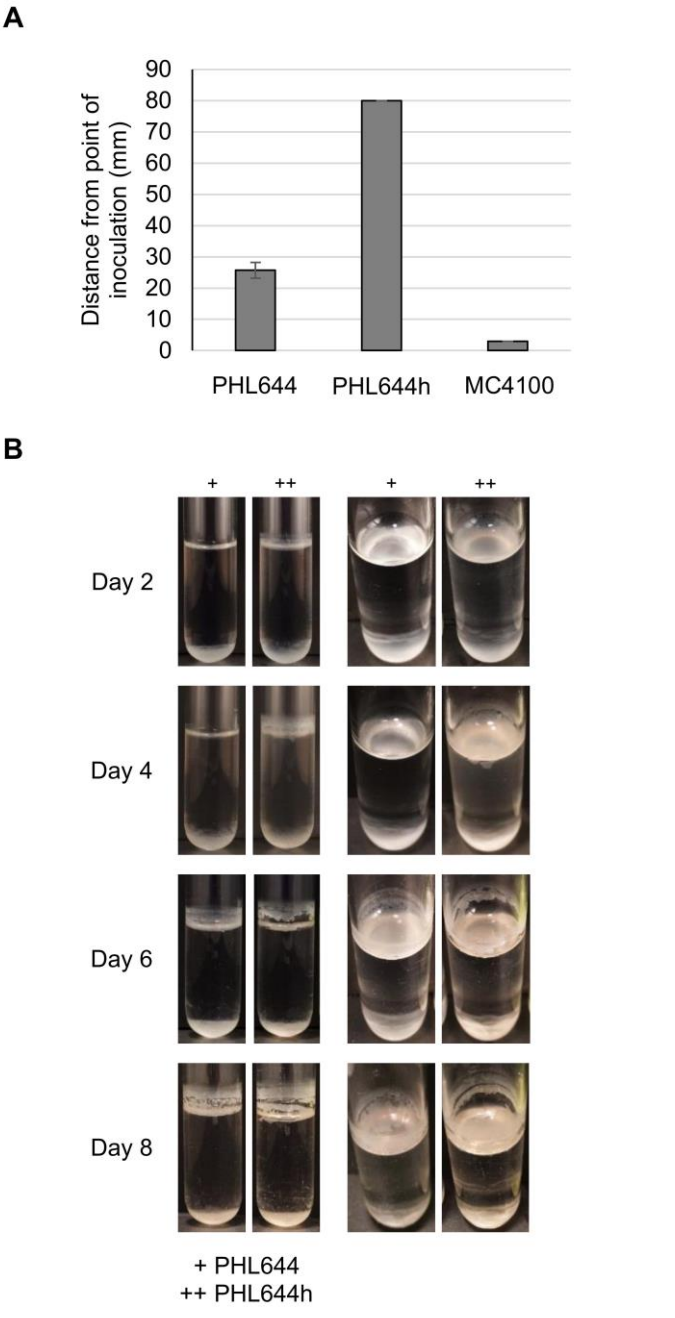
A
Distance from point of inoculation (mm)
90
80
70
60
50
40
30
20
10
0
PHL644
PHL644h
MC4100
B
+
++
+
++
Day 2
Day 4
Day 6
Day 8
+ PHL644
++ PHL644h
C
PHL644
Static 8 days
70rpm 1 day Static 7 days
70 rpm 8 days
D
PHL644h
Static 8 days

FIGURE 3

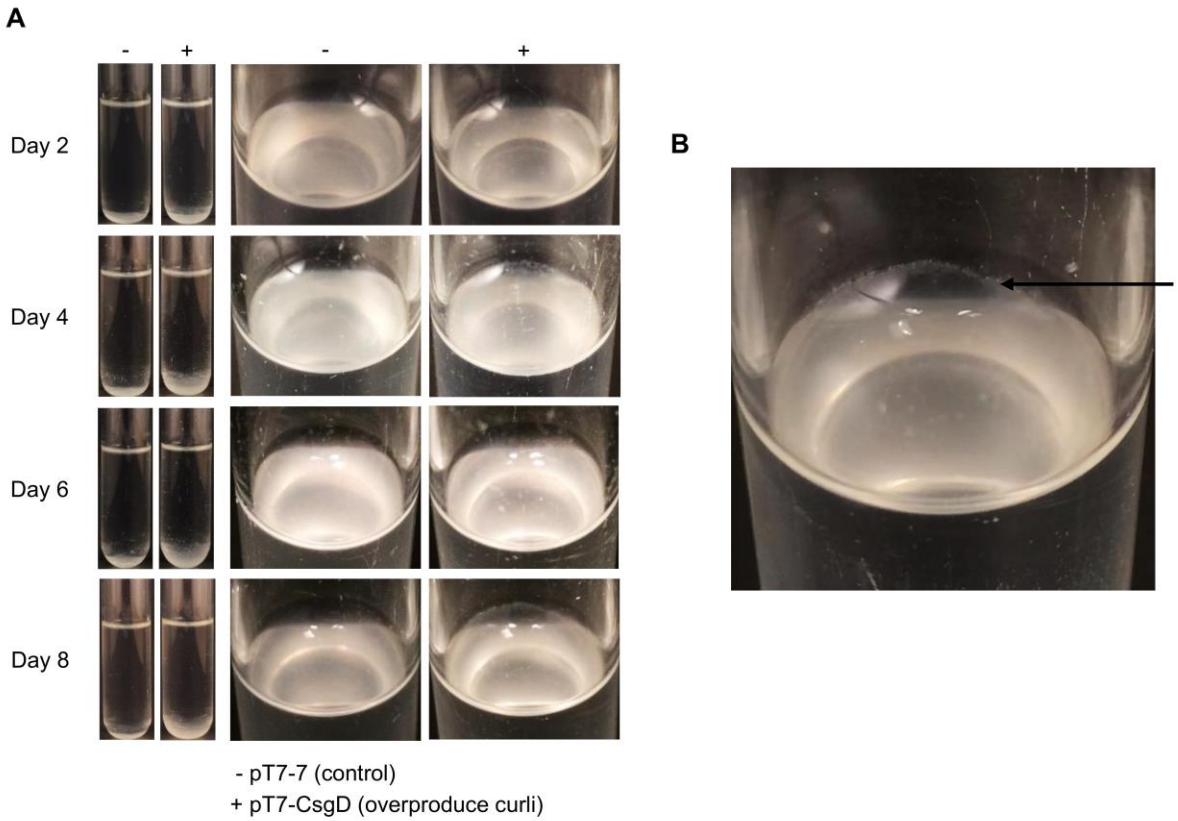
A
-
+
-
+
Day 2
Day 4
Day 6
Day 8
- pT7-7 (control)
+ pT7-CsgD (overproduce curli)
B

FIGURE 4

A

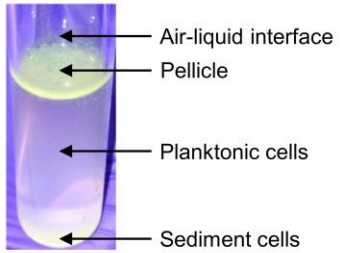

Comparison	Day 1	Day 2	Day 3
Pellicle to Interface	*	*	*
Pellicle to Planktonic	NS	NS	NS
Pellicle to Sediment	NS	*	*
Interface to Planktonic	*	NS	*
Interface to Sediment	NS	NS	NS
Planktonic to Sediment	*	NS	*

B

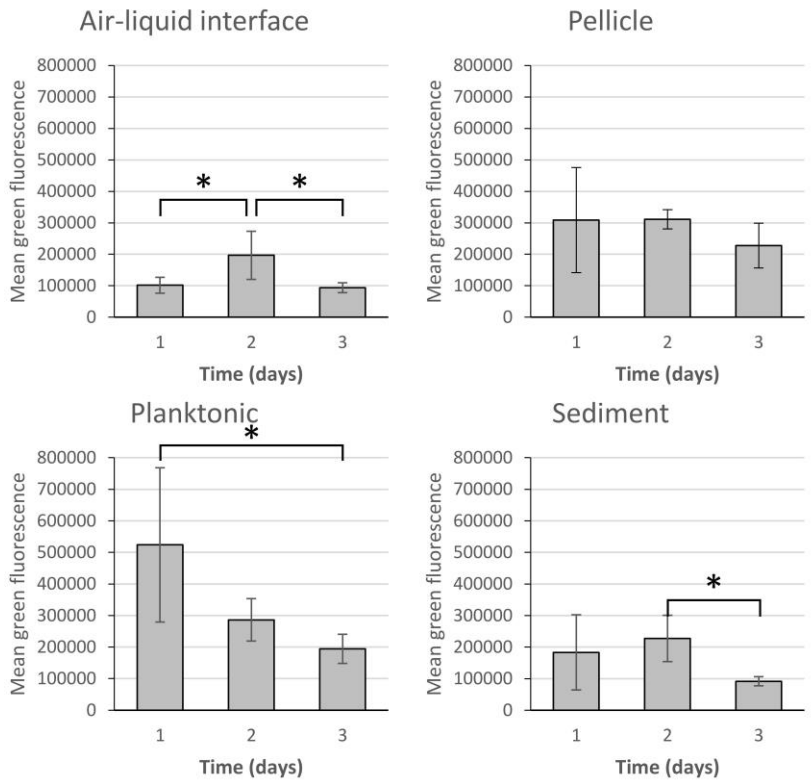

FIGURE 5

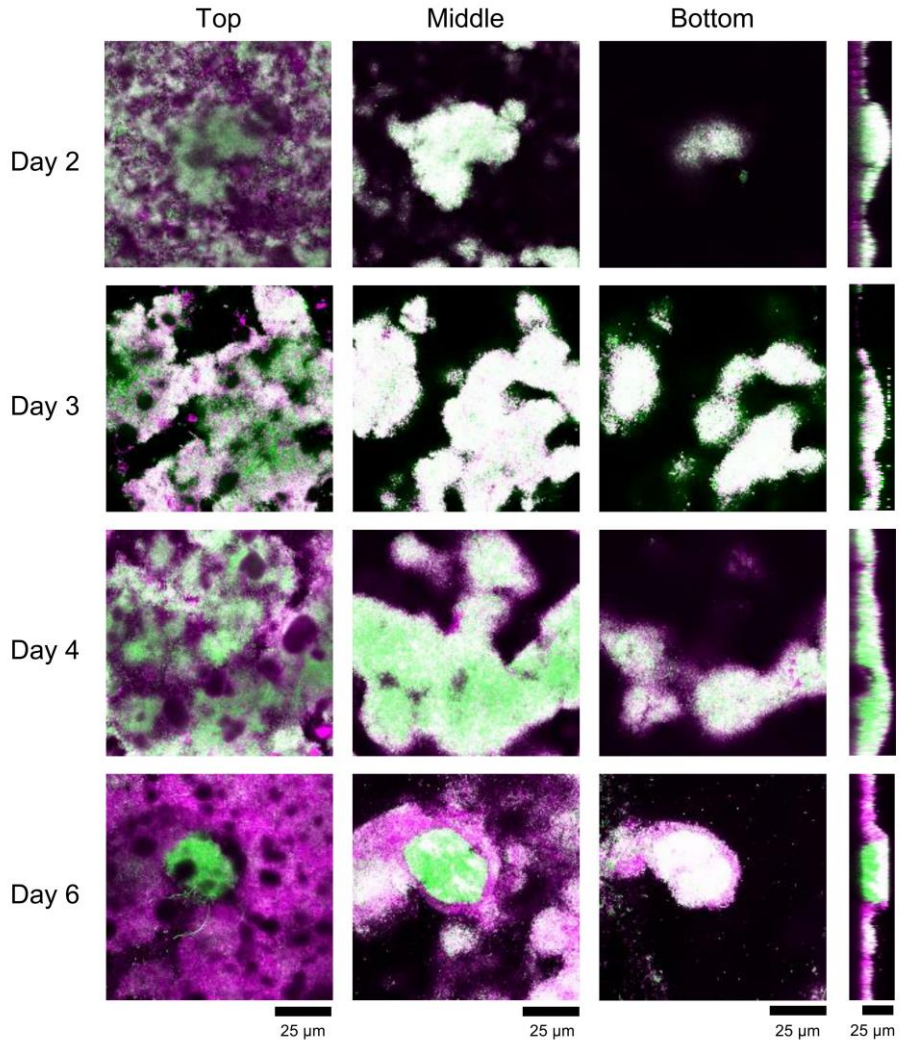

FIGURE 6

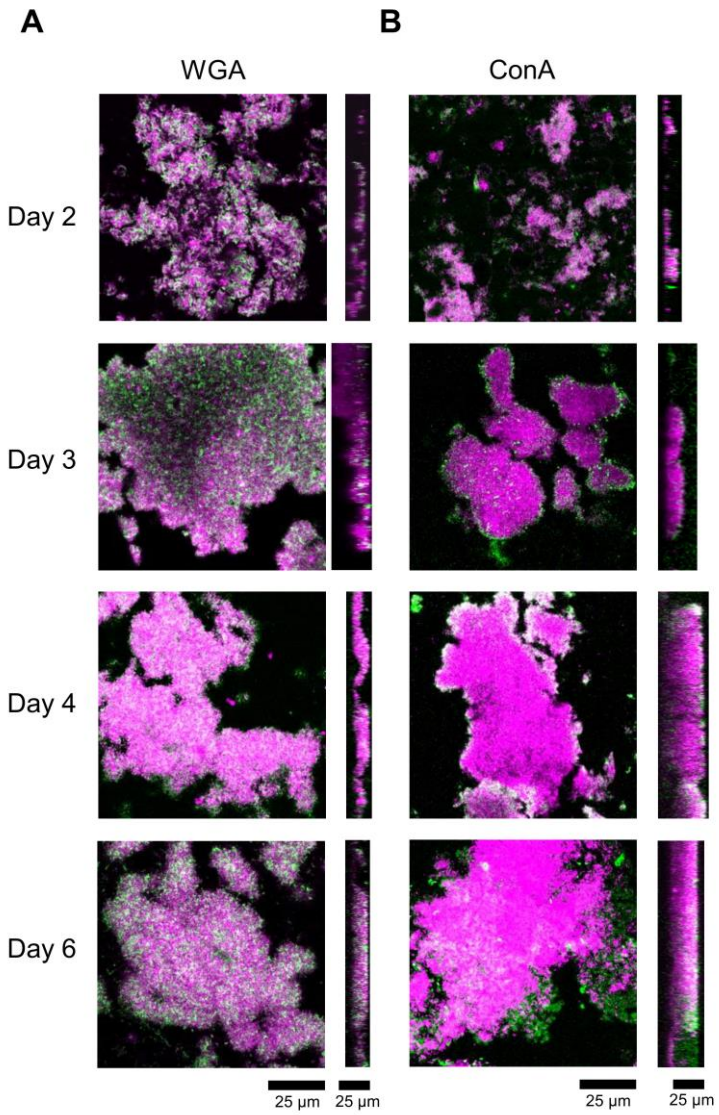

SUPPLEMENTARY INFORMATION for

Pellicle formation by *Escherichia coli* K-12: role of adhesins and motility

Stacey R Golub, Tim W Overton*

School of Chemical Engineering, College of Engineering and Physical Sciences and Institute of Microbiology and Infection, University of Birmingham, Edgbaston, Birmingham, B15 2TT, UK.

*to whom correspondence should be addressed: t.w.overton@bham.ac.uk, +44 (0) 121 414 5306

Supplementary methods

DNA genome sequencing

Genomes of strains PHL644 and PHL644h were sequenced by microbesNG (https://microbesng.uk/). Strains PHL644 and PHL644h were grown on nutrient agar plates and supplied to microbesNG on beads. Three beads were washed with extraction buffer containing lysozyme and RNase A, incubated for 25 min at 37 °C. Proteinase K and RNaseA were added and incubated for 5 min at 65 °C. Genomic DNA was purified using an equal volume of SPRI beads and resuspended in EB buffer.

DNA was quantified in triplicates with the Quantit dsDNA HS assay in an Ependorff AF2200 plate reader. Genomic DNA libraries were prepared using Nextera XT Library Prep Kit (Illumina, San Diego, USA) following the manufacturer's protocol with the following modifications: two nanograms of DNA instead of one were used as input, and PCR elongation time was increased to 1 min from 30 seconds. DNA quantification and library preparation were carried out on a Hamilton Microlab STAR automated liquid handling system. Pooled libraries were quantified using the Kapa Biosystems Library Quantification Kit for Illumina on a Roche light cycler 96 qPCR machine. Libraries were sequenced on the Illumina HiSeq using a 250bp paired end protocol.

Reads were adapter trimmed using Trimmomatic 0.30 with a sliding window quality cutoff of Q15 (Bolger *et al*., 2014). De novo assembly was performed on samples using SPAdes version 3.7 (Bankevich *et al*., 2012), and contigs were annotated using Prokka 1.11 (Seeman, 2014). Variant calling was performed using VarScan (Koboldt *et al*., 2009) using the following parameters: minimum coverage 3, minimum variant frequency 10%, p-value 0.05.

References for supplemental methods

Bolger, A. M., Lohse, M., & Usadel, B. (2014). Trimmomatic: a flexible trimmer for Illumina sequence data. Bioinformatics, 30(15), 2114–2120.

Bankevich, A., Nurk, S., Antipov, D., Gurevich, A. A., Dvorkin, M., Kulikov, A. S., & Pevzner, P. A. (2012). SPAdes: A New Genome Assembly Algorithm and Its Applications to Single-Cell Sequencing. Journal of Computational Biology, 19(5), 455–477.

Seemann T (2014) Prokka: rapid prokaryotic genome annotation. *Bioinformatics*. 30(14):2068-9

Koboldt DC, Chen K, Wylie T, Larson DE, McLellan MD, Mardis ER, Weinstock GM, Wilson RK, & Ding L (2009). VarScan: variant detection in massively parallel sequencing of individual and pooled samples. *Bioinformatics,* **25**(17): 2283-5

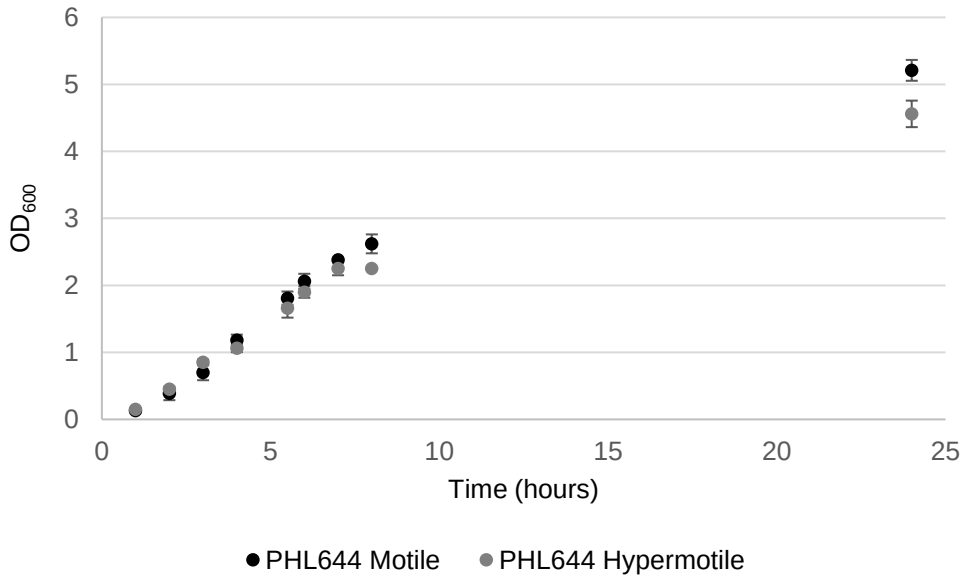

Supplemental Figure S1. Growth Curve of PHL644 and PHL644h in LB medium over 24 hours.

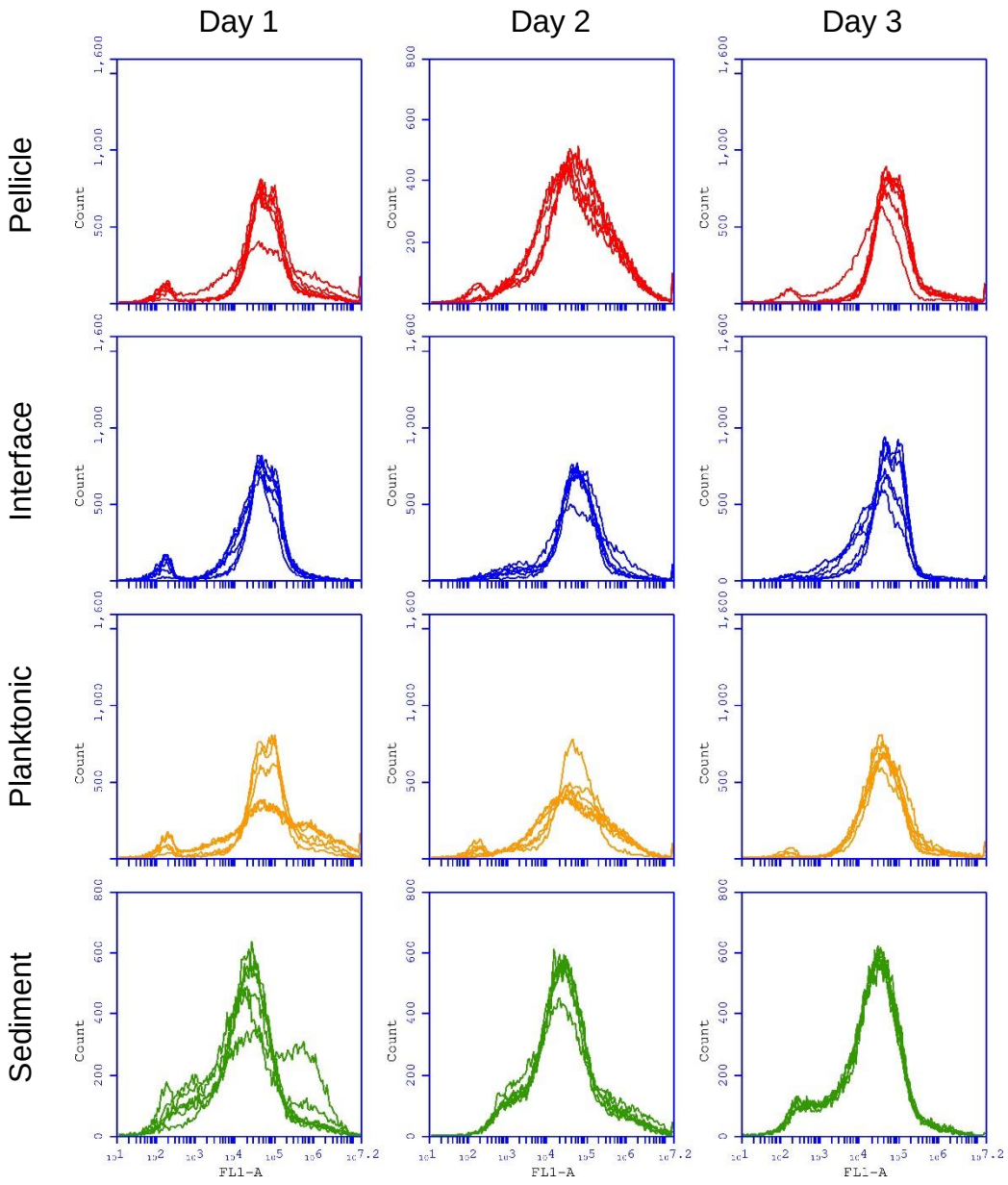

Supplemental Figure S2. Green fluorescence histograms corresponding to data in Fig. 4B.

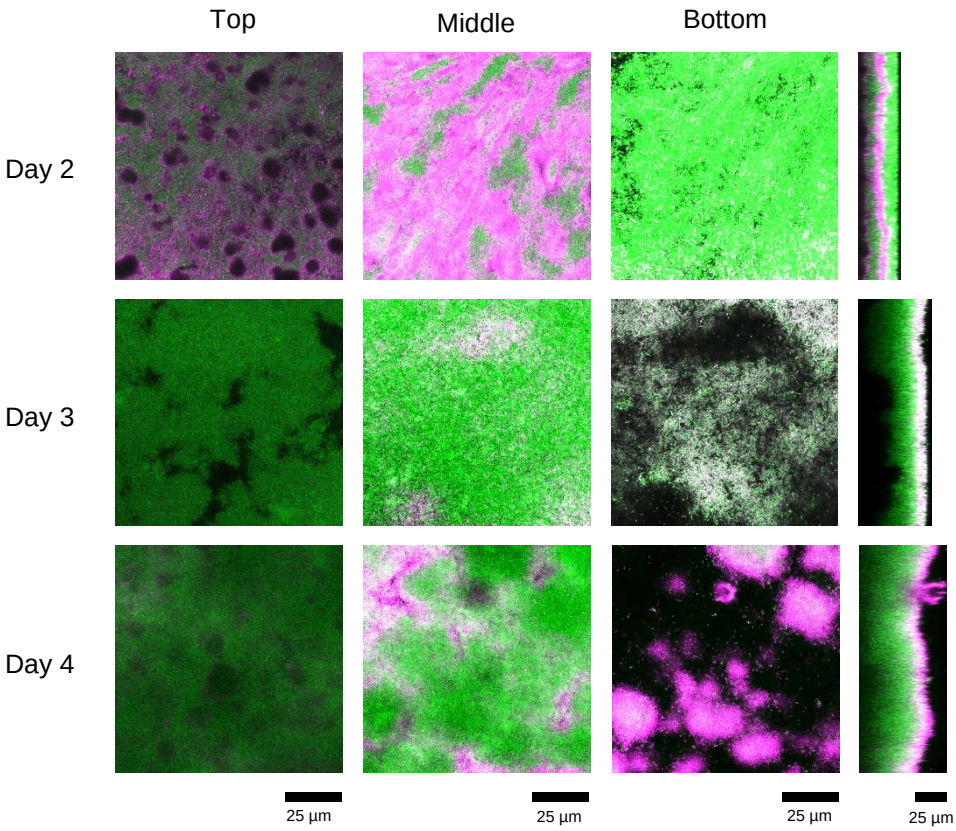

Supplemental Figure S3. Visualisation of PHL644h curli production by confocal microscopy. *E. coli* PHL644h pJLC-T was grown in M63+ medium at 30 °C and 70 rpm for four days and pellicles were harvested, stained with DNA stain SYTO62 (magenta) and visualised by confocal microscopy on days 2, 3, and 4; green represents GFP. Representative single plane images are from the top (air-facing), middle, and bottom (media-facing) of each pellicle as well as the side-view are shown.

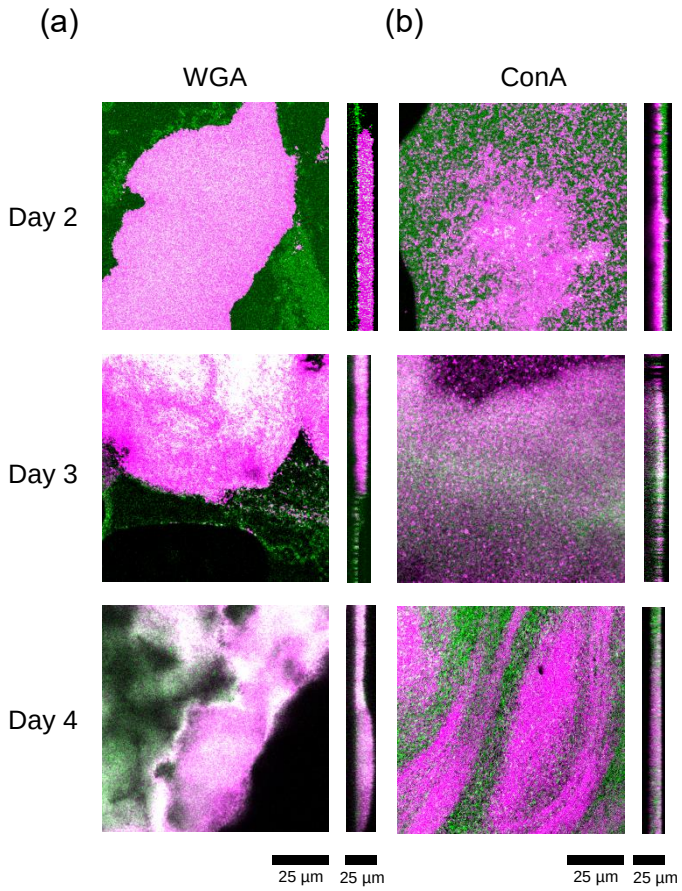

Supplemental Figure S4. Visualisation of PHL644h EPS production by confocal microscopy. *E. coli* PHL644h was grown in M63+ medium at 30 °C and 70 rpm for four days, pellicles were harvested and stained with DNA stain SYTO62 (magenta) and either (a) WGA-FITC (stains PNAG, shown as green) or (b) ConA-Alexa Fluor 488 (stains colonic acid, shown as green) and visualised by confocal microscopy on days 2, 3 and 4. Representative single plane images from each pellicle as well as the side view are shown.

Supplemental Table S1. Mutations in PHL644 and PHL644h.

Position	Ref Allele Forward Strand	Alt Allele Fwd Strand	Average Depth	No calls	Homozygous calls	Het calls	Mutation Type	Mutation Strength	Mutation Type2	Codon Substitution	Amino Acid Substitution	Locus Tag	Gene	PHL644h	PHL644	Discriminatory	Maximum Frequency	Comments
75949	G	A	82	0	1	1	SYNONYMOUS CODING	LOW	SILENT	agC/agT	S450	BN896_RS00350	HTH-type transcriptional regulator *sgrR*	A	G/A	Y	78.12	Silent mutations
75952	C	T	81	0	1	1	SYNONYMOUS CODING	LOW	SILENT	gaG/gaA	E449			T	C/T	Y	77.42	
276948	G	A	85	0	0	1							upstream of *mhpT*	G/A		Y	13.64	No evidence in literature to link to motility or biofilms
276955	T	C	81	0	0	1								T/C		Y	10.94	
276956	G	A	82	0	0	1								G/A		Y	13.85	
276962	T	C	85	0	0	1								T/C		Y	13.43	
276969	T	C	87	0	0	1								T/C		Y	13.43	
276976	AGAC	A	86	0	0	1								AGAC/A		Y	13.64	
276986	GCGT	G	79	0	0	1								GCGT/G		Y	15.25	
277005	CG	C	81	0	0	1								CG/C		Y	13.33	
277029	A	G	96	0	0	1								A/G		Y	13.11	
277050	A	G	93	0	0	1								A/G		Y	14.29	
277105	GC	G	85	0	0	1								GC/G		Y	12.31	
277113	C	T	88	0	0	1								C/T		Y	20	
277130	A	G	98	0	0	1									A/G	Y	15.08	
277151	G	A	92	0	0	1									G/A	Y	10.43	

410583	T	C	89	0	0	1							intergentic region		T/C	Y	11.3	Between the ends of two genes - *higA* family addiction module antidote protein - and copper-exporting P-type ATPase *copA*
480792	T	C	158	0	1	1	NON SYNONYMOUS CODING	MODERATE	MISSENSE	Aca/Gca	T29A	BN896_RS02400	Prophage DLP12 serum resistance lipoprotein *borD*	T/C	C	Y	75.54	DLP12 removal deletion leads to decreased biofilm formation in *E. coli* K-12. (Wang *et al.* 2010)
480794	T	G	157	0	1	1	NON SYNONYMOUS CODING	MODERATE	MISSENSE	cAg/cCg	Q28P			T/G	G	Y	75.96	
886558	T	TG	85	0	0	1	FRAME SHIFT	HIGH		cgg/Gcgg	R27A?	BN896_RS24500	Hypothetical		T/TG	Y	10.09	No evidence in literature to link to motility or biofilms
886566	G	A	86	0	0	1	NON SYNONYMOUS CODING	MODERATE	MISSENSE	Gag/Aag	E29K				G/A	Y	10.09	
1156894	C	T	55	0	0	1	NON SYNONYMOUS CODING	MODERATE	MISSENSE	Ggc/Agc	G29S	BN896_RS05760	Small toxic polypeptide *ldrB*	C/T		Y	15.91	No evidence in literature to link to motility or biofilms
1318309	A	G	178	0	1	1	SYNONYMOUS CODING	LOW	SILENT	gaA/gaG	E244	BN896_RS23165	*stfR* - Rac prophage side tail fiber protein	A/G	G	Y	76.17	Rac removal and also *stfR* deletion led to decreased biofilm formation in *E. coli* K-12 in M9C medium. (Wang *et al.* 2010) *stfR* mutant made more biofilm in LB glucose medium than wt (Domka 2007) Rac removal led to increased biofilm formation in K-12 in LB and M9C-glu. (Liu et al. 2015) Rac removal led to increased motility in *E. coli* K-12 (Liu et al. 2015). This effect was shown to be not caused by IS insertion at *flhDC.*
1318312	G	A	181	0	1	1	SYNONYMOUS CODING	LOW	SILENT	gcG/gcA	A245			G/A	A	Y	75.52	
1318380	G	A	190	0	1	1	NON SYNONYMOUS CODING	MODERATE	MISSENSE	gGa/gAa	G268E			G/A	A	Y	75.21	
1318417	C	T	180	0	1	1	SYNONYMOUS CODING	LOW	SILENT	aaC/aaT	N280			C/T	T	Y	75	
1320595	A	T	116	0	0	1	SYNONYMOUS CODING	LOW	SILENT	gcA/gcT	A1006			A/T		Y	12.22	
1320599	A	G	135	0	0	1	NON SYNONYMOUS CODING	MODERATE	MISSENSE	Aca/Gca	T1008A			A/G		Y	12.38	
1320601	A	T	137	0	0	1	SYNONYMOUS CODING	LOW	SILENT	acA/acT	T1008			A/T		Y	11.93	
1320608	G	C	128	0	0	1	NON SYNONYMOUS CODING	MODERATE	MISSENSE	Gtg/Ctg	V1011L			G/C		Y	12.38	

1321149	T	C	78	0	0	1	SYNONYMOUS CODING	LOW	SILENT	gaT/gaC	D70	BN896_RS06650	*tfrA* - Rac prophage tail fiber assembly protein	T/C		Y	12.9	
1354730	T	C	87	0	0	1	SYNONYMOUS CODING	LOW	SILENT	ggT/ggC	G270	BN896_RS06795	Hypothetical	T/C		Y	16.46	Silent mutations
1354739	G	A	85	0	0	1	SYNONYMOUS CODING	LOW	SILENT	gcG/gcA	A273			G/A		Y	18.42	
1354799	C	T	78	0	0	1	SYNONYMOUS CODING	LOW	SILENT	atC/atT	I293			C/T		Y	12.12	
1421790	A	C	58	0	0	1	NON SYNONYMOUS CODING	MODERATE	MISSENSE	aaA/aaC	K70N	BN896_RS07110	*pptA*	A/C		Y	12	No evidence in literature to link to motility or biofilms
2420909	T	C	29	0	0	1	NON SYNONYMOUS CODING	MODERATE	MISSENSE	Ttt/Ctt	F58L	BN896_RS24710	Hypothetical	T/C		Y	19.35	No evidence in literature to link to motility or biofilms
2420911	T	G	28	0	0	1	NON SYNONYMOUS CODING	MODERATE	MISSENSE	ttT/ttG	F58L			T/G		Y	16.67	
2742602	G	T	12	0	1	1							upstream of 23S rRNA	T	G/T	Y	90.91	No evidence in literature to link to motility or biofilms
2742607	C	T	12	0	1	1							upstream of 23S rRNA	T	C/T	Y	90	
2841331	T	C	4	0	1	0							Upstream of *rbsR*		C	Y	100	RbsR is a pleiotrpoic regulator of motility in *Serratia* (Lee *et* al., 2017).
3177000	A	G	43	0	0	1							Upstream of *ftsY*		A/G	Y	12	No evidence in literature to link to motility or biofilms
3336379	C	T	61	0	0	1	NON SYNONYMOUS CODING	MODERATE	MISSENSE	tCt/tTt	S105F	BN896_RS16450	30S ribosomal protein S8	C/T		Y	13.33	No evidence in literature to link to motility or biofilms
3355811	TCGAAA	T	78	0	0	1							Upstream of 23S rRNA	TCGAAA/T		Y	17.31	No evidence in literature to link to motility or biofilms
4427131	A	C	34	0	0	1	SYNONYMOUS CODING	LOW	SILENT	acA/acC	T69	BN896_RS21900	IS1 family transposase		A/C	Y	11.11	Silent mutation

2

References from Supplemental Table S1

Wang X, Kim Y, Ma Q, Hong SH, Pokusaeva K, Sturino JM, Wood TK. (2010) Cryptic prophages help bacteria cope with adverse environments. *Nat Commun*. **1**:147. doi: 10.1038/ncomms1146.

Liu X, Li Y, Guo Y, Zeng Z, Li B, Wood TK, Cai X, Wang X. (2015) Physiological Function of Rac Prophage During Biofilm Formation and Regulation of Rac Excision in *Escherichia coli* K-12. *Sci Rep*. **5**:16074. doi: 10.1038/srep16074.

Domka J, Lee J, Bansal T, Wood TK. (2007) Temporal gene-expression in *Escherichia coli* K-12 biofilms. *Environ Microbiol*. **9**:332-46.

Lee CM, Monson RE, Adams RM, Salmond GPC. (2017) The LacI-Family Transcription Factor, RbsR, Is a Pleiotropic Regulator of Motility, Virulence, Siderophore and Antibiotic Production, Gas Vesicle Morphogenesis and Flotation in *Serratia*. *Front Microbiol*. **8**:1678. doi: 10.3389/fmicb.2017.01678.